VNU Journal of Science, Earth Sciences 24 (2008) 213-223

Potential evapotranspiration estimation and its effect on hydrological model response at the Nong Son Basin

Vu Van Nghi[1,*], Do Duc Dung[2], Dang Thanh Lam[2]

[1] *State Key Laboratory of Hydrology, Water Resources and Hydraulic Engineering, Hohai University, China*

[2] *Southern Institute for Water Resources Planning, Ho Chi Minh City*

Received 4 November 2008; received in revised form 28 November 2008.

Abstract. The potential evapotranspiration can be directly calculated by the Penman-Monteith equation, known as the one-step method. The approach requires data on the land cover and related-vegetation parameters based on AVHRR and LDAS information, which are available in recent years. The Nong Son Basin, a sub-catchment of the Vu Gia - Thu Bon Basin in the Central Vietnam, is selected for this study. To this end, NAM model was used; the obtained results show that the NAM model has a potential to reproduce the effects of potential evapotranspiration on hydrological response. This is seemingly manifested in the good agreement between the model simulation of discharge and the observed at the stream gauge.

Keywords: Potential evapotranspiration; Penman-Monteith method; Piche evaporation; Leaf area index (LAI); Normalized difference vegetation index (NDVI).

1. Introduction

One of the key inputs to hydrological modeling is potential evapotranspiration, which refers to the maximum meteorologically evaporative power on land surface. Two kinds of potential evapotranspiration are necessary to be defined: either from the interception or from the root zone when the interception is exhausted but soil water is freely available, specifically at field capacity [11, 32]. The actual evapotranspiration is distinguished from the potential through the limitations imposed by the water deficit. Evapotranspiration can be directly measured by lysimeters or eddy correlation method, but it is expensive and thus practical only in researches over a plot for a short time. The pan or Piche evaporation has long records with dense measurement sites. However, to apply it in hydrological models, first, a pan/Piche coefficient K_p, and then a crop coefficient K_c must be multiplied as well. Due to the difference on sitting and weather conditions, K_p is often expressed as a function of local environmental variables such as wind speed, humidity, upwind fetch, etc. A global equation of K_p is still unavailable. The values of K_c from the literature are empirical, most for agricultural crops, and subjectively selected. Moreover, the observed Piche data show some erroneous results which are difficult to explain [4], and the pan evaporameter is considered to be inaccurate [8, 10]. On the other hand, a great

* Corresponding author. Tel.: 0086-1585056977.
E-mail: vuvannghi@yahoo.com

number of evaporation models has been developed and validated, from the single climatic variable driven equations [29] to the energy balance and aerodynamic principle combination methods [23]. Among them, probably the Penman equation is the most physically sound and rigorous. Monteith [20] generalized the Penman equation for water-stressed crops by introducing a canopy resistance. Now the Penman-Monteith model is widely employed.

As a result, in this study the Penman-Monteith method is selected to compute directly potential evapotranspiration according to the vegetation dataset at 30s resolution based on AVHRR (Advanced Very High Resolution Radiometer) and LDAS (Land Data Assimilation System) information for the Nong Son catchment. To assess the suitability of this approach, the conceptual rainfall-runoff model known as NAM [8] is used to examine its effect on hydrological response.

2. Potential evapotranspiration model description

2.1. Penman-Monteith equation

Potential evapotranspiration can be calculated directly with the Penman-Monteith equation [3] as follows:

$$\lambda ET = \frac{\Delta(R_n - G) + \rho_a c_p \dfrac{(e_s - e_a)}{r_a}}{\Delta + \gamma\left(1 + \dfrac{r_s}{r_a}\right)}, \qquad (1)$$

where ET is the evapotranspiration rate (mm.d^{-1}), λ is the latent heat of vaporization (= 2.45 MJ.kg^{-1}), R_n is the net radiation, G is the soil heat flux (with a relatively small value, in general, it may be ignored), e_s is the saturated vapor pressure, e_a is the actual vapor pressure, (e_s - e_a) represents the vapour pressure deficit of the air, ρ_a is the mean air density at constant pressure, c_p is the specific heat of the air (= 1.01 kJ.kg^{-1}.K^{-1}), Δ represents the slope of the saturation vapour pressure temperature relationship, γ is the psychrometric constant, and r_s and r_a are the (bulk) surface and aerodynamic resistances.

The Penman-Monteith approach as formulated above includes all parameters that govern energy exchange and corresponding latent heat flux (evapotranspiration) from uniform expanses of vegetation. Most of the parameters are measured, or can be readily calculated from weather data. The equation can be utilized for the direct calculation of any crop evapotranspiration as the surface and aerodynamic resistances are crop specific.

2.2. Factors and parameters determining ET

2.2.1. Land surface resistance parameterization

a. Aerodynamic resistance

The rate of water vapor transfer away from the ground by turbulent diffusion is controlled by aerodynamic resistance r_a, (s.m^{-1}) which is inversely proportional to wind speed and changes with the height of the vegetation covering the ground, as:

$$r_a = \frac{\ln[(z_u - d)/z_{om}]\ln[(z_e - d)/z_{oh}]}{\kappa^2 u_z}, \qquad (2)$$

where z_u is the height of wind measurements (m); z_e is the height of humidity measurements; d is the zero plane displacement height (m); z_{om} is the roughness length governing momentum transfer (m); z_{oh} is the roughness length governing transfer of heat and vapour (m); u_z is the wind speed; and κ is the von-Karman constant (= 0.41).

Many studies have explored the nature of the wind regime in plant canopies. d and z_{om} have to be considered when the surface is covered by vegetation. The factors depend upon the crop height and architecture. Several empirical equations [6, 12, 21, 31] for estimating d, z_{om} and z_{oh} have been developed. In this study, the estimate can be made of r_a by assuming [5] that $z_{om} = 0.123\ h_c$ and $z_{oh} = 0.0123\ h_c$, and [21] that $d = 0.67\ h_c$, where h_c (m) is the mean height of the crop.

b. Surface resistance

The "bulk" surface resistance describes the resistance of vapor flow through transpiring crop and evaporating soil surface. Where the vegetation does not completely cover the soil, the resistance factor should indeed include the effects of the evaporation from the soil surface. If the crop is not transpiring at a potential rate, the resistance depends also on the water status of the vegetation. An acceptable approximation [1, 3] to a much more complex relation of the surface resistance of fully dense cover vegetation is:

$$r_s = \frac{r_l}{LAI_{active}}, \tag{3}$$

where r_l is the bulk stomatal resistance of the well-illuminated (s.m^{-1}), and LAI_{active} is the active (sunlit) leaf area index (m^2 leaf area over m^2 soil surface).

A general equation for LAI_{active} is [2, 16, 30]:

$$LAI_{active} = 0.5 LAI \tag{4}$$

The bulk stomatal resistance r_l is the average resistance of an individual leaf. This resistance is crop specific and differs among crop varieties and crop management. It usually increases as the crop ages and begins to ripen. There is, however, a lack of consolidated information on changes in r_l over the time for different crops. The information available in the literature on stomatal resistance is often oriented towards physiological or ecophysiological studies. The stomatal resistance is influenced by climate and by water availability. However, the influences vary from one crop to another and different varieties can be affected differently. The resistance increases when the crop is water stressed and the soil water availability limits crop evapotranspiration. Some studies [14, 15, 19, 33] indicate that stomatal resistance is influenced to some extent by radiation intensity, temperature and vapor pressure deficit.

If the crop is amply supplied with water, the crop resistance r_s reaches a minimum value, known as the *basis canopy resistance*. The transpiration of the crop is then maximum and referred to as potential transpiration. The relation between r_s and the pressure head in the root zone is crop dependent. Minimum values of r_s range from 30 s.m^{-1} for arable crops to 150 s.m^{-1} for forest. For grass a value of 70 s.m^{-1} is often used [10]. It should be noted that r_s cannot be measured directly, but has to be derived from the Penman-Monteith formula where *ET* is obtained from, for example, the water balance of a lysimeter.

The Leaf Area Index (*LAI*), a dimensionless quantity, is the leaf area (upper side only) per unit area of soil below it. The active *LAI* is the index of the leaf area that actively contributes to the surface heat and vapor transfer. It is generally the upper, sunlit portion of a dense canopy. The *LAI* values for various crops differ widely but values of 3-5 are common for many mature crops. For a given crop, the green *LAI* changes throughout the season and normally reaches its maximum before or at flowering. *LAI* further depends on the plant density and the crop variety. Several studied and empirical equations [19, 31] for the estimate of *LAI* have been developed. If h_c is the mean height of the crop, then the *LAI* can be estimated by [1]:

$$\begin{aligned} &LAI = 24h_c \\ &LAI = 5.5 + 1.5\ln(h_c) \\ &(\text{clipped grass with } 0.05 < h_c < 0.15\,\text{m}) \\ &(\text{alfalfa with } 0.10 < h_c < 0.50\,\text{m}) \end{aligned} \tag{5}$$

As an alternative, the spectral vegetation indices from satellite-based spectral observations, such as *NDVI* (normalized difference vegetation index), or simple ratio ($SR = (1 + NDVI)/(1 - NDVI)$); are widely used to extract vegetation biophysical parameters of which *LAI* is the most important. The use of monthly vegetation index is a good way to take into account the phenological development of the *LAI*, as well as the effects of prolonged water stresses that reduce the *LAI* [18]. In this study, the monthly maximum composite 1-km resolution *NDVI* dataset obtained from NOAA-AVHRR (National Oceanic and Atmospheric Administration - Advanced very High Resolution Radiometer) in 1992, 1995, and 1996 years were used to estimate *LAI*. The simple relationships between *LAI* and *NDVI* were taken from SiB2 [25]. For evenly distributed vegetation, such as grass and crops:

$$LAI = LAI_{\max}\frac{\ln(1-FPAR)}{\ln(1-FPAR_{\max})}. \tag{6}$$

For clustered vegetation, such as coniferous trees and shrubs:

$$LAI = \frac{LAI_{\max}FPAR}{FPAR_{\max}}, \tag{7}$$

where $FPAR$ is the fraction of photosynthetically active radiation absorbed by the canopy, which is calculated as:

$$FPAR = \frac{(SR-SR_{\min})(FPAR_{\max}-FPAR_{\min})}{SR_{\max}-SR_{\min}}, \tag{8}$$

where $FPAR_{max}$ and $FPAR_{min}$ are taken as 0.950 and 0.001, respectively. SR_{max} and SR_{min} are SR values corresponding to 98 and 5% of *NDVI* population, respectively.

Land cover classes of needleleaf deciduous, evergreen and shrub land thicket are treated as clumped vegetation types [24]. In the cases, where there is a combination of clustered and evenly distributed vegetation, LAI can be calculated by a combination of equations (6) and (7):

$$LAI = (1-F_{cl})LAI_{\max}\frac{\ln(1-FPAR)}{\ln(1-FPAR_{\max})} + F_{cl}\frac{LAI_{\max}FPAR}{FPAR_{\max}} \tag{9}$$

where F_{cl} is the fraction of clumped vegetation in the area.

2.2.2. Surface exchanges

a. Saturated vapor content of air

The saturated vapor pressure is related to temperature; if e_s is in kilopascals (kPa) and T is in degrees Celsius (°C), an approximate equation is [28]:

$$e_s = 0.6108\exp\left(\frac{17.27T}{237.3+T}\right). \tag{10}$$

It is important in building physically based models of evaporation that not only e_s is a known function of temperature, but so is Δ (kPa.C^{-1}), the gradient of this function, de_s/dT. This gradient is given by:

$$\Delta = \frac{4098e_s}{(237.3+T)^2}. \tag{11}$$

The relative humidity (RH %) expresses the degree of saturation of the air as a ratio of the actual (e_a) to the saturation (e_s) vapor pressure at the same temperature (T):

$$RH = 100\frac{e_a}{e_s}. \tag{12}$$

b. Sensible heat

The density of (moist) air can be calculated from the ideal gas laws, but it is adequately estimated from:

$$\rho_a = 3.486\frac{P}{275+T}, \tag{13}$$

where P is the atmospheric pressure in kPa. Assuming 20°C is the standard temperature of atmosphere, P as a function of height z (in meters) above the mean sea level can be employed to calculate by:

$$P = 101.3\times\left(\frac{293-0.0065z}{293}\right)^{5.26}. \tag{14}$$

c. Psychrometric constant

The psychrometric constant γ (kPa °C^{-1}) is given by:

$$\gamma = \frac{c_pP}{\varepsilon\lambda} = 0.665\times10^{-3}P, \tag{15}$$

where ε is the ratio the molecular weights of water vapor and dry air, equals to 0.622. Other parameters in the equation are defined above.

2.2.3. Radiation balance at land surface

In the absence of restrictions due to water availability at the evaporative surface, the amount of radiant energy captured at the earth's surface is the dominant control on regional evaporation rates. As a monthly average, the radiant energy at the ground may be the most "portable" meteorological variable involved in evaporation estimation, in the sense that it is driven by the astronomical rather than the local climate conditions. Understanding the surface radiation balance, and how to quantify it, is therefore crucial to understanding and quantifying evaporation.

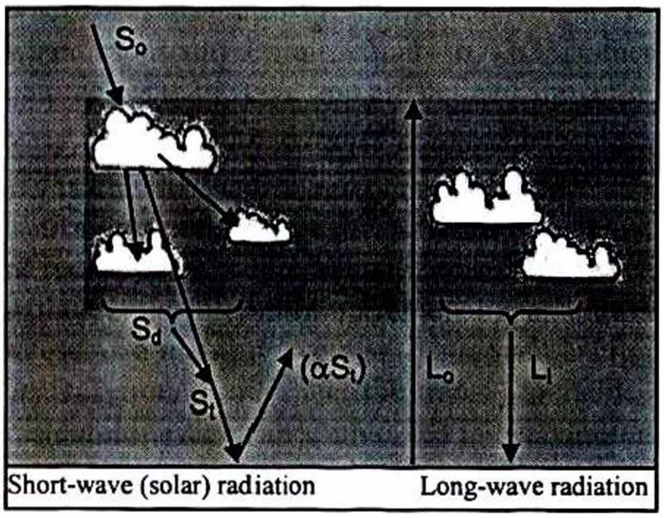

Fig. 1. Radiation balance at the Earth's surface.

a. Net short wave radiation

The net short wave radiation S_n ($MJ.m^{-2}.day^{-1}$) is the portion of the incident short wave radiation captured at the ground taking into account losses due to reflection, and given by:

$$S_n = S_t(1-\alpha), \tag{16}$$

where α is the reflection coefficient or albedo; and S_t is the solar radiation ($MJ.m^{-2}.day^{-1}$).

The values of albedo for broad land cover classes are given in various scientific literatures. The solar radiation S_t ($MJ.m^{-2}.day^{-1}$) in most of the cases can be estimated [7] from measured sunshine hours according to the following empirical relationship:

$$S_t = \left(a_s + b_s \frac{n}{N}\right) S_0, \tag{17}$$

where S_0 is the extraterrestrial radiation ($MJ.m^{-2}.day^{-1}$); a_s is the fraction of S_0 on overcast days ($n = 0$); ($a_s + b_s$) is the fraction of S_0 on clear days (for average climates $a_s = 0.25$ and $b_s = 0.50$); n is the bright sunshine hours per day (h); N is the total day length (h); and n/N is the cloudiness fraction. The values of N and S_0 for different latitudes are given in various handbooks [3, 10].

b. Net long wave radiation

The exchange of long wave radiation L_n ($MJ.m^{-2}.day^{-1}$) between vegetation and soil on the one hand, and atmosphere and clouds on the other, can be represented by the following radiation law [3, 10, 17]:

$$L_n = \sigma\left(0.9\frac{n}{N}+0.1\right)\left(0.34-0.14\sqrt{e_a}\right)(T+273)^4 \tag{18}$$

where σ is the Stefan-Boltzmann constant (4.903×10^{-9} $MJ.m^{-2}.K^{-4}.day^{-1}$).

c. Net radiation

The net radiation R_n is the difference between the incoming net short wave radiation S_n and the outgoing net long wave radiation L_n:

$$R_n = S_n - L_n \tag{19}$$

Using the indicative values given in the previous sections, for general purposes when only sunshine, temperature, and humidity data are available, net radiation (in $MJ.m^{-2}.day^{-1}$) can be estimated by the following equation:

$$R_n = \left(0.25 + 0.5\frac{n}{N}\right)S_0 - \left(0.9\frac{n}{N} + 0.1\right) \left(0.34 - 0.14\sqrt{e_a}\right)(T+273)^4 \sigma \tag{20}$$

3. Study area and data processing

3.1. Study area description

The study area (14°41'-15°45'N and 107°40'-108°20'E) covers 3,160 km² with the gauging station at Nong Son. It is a mountainous sub-basin of the Vu Gia - Thu Bon Basin located in the East of Truong Son mountain range in the Central Vietnam (Fig. 2.a). The altitude ranges from several meters to 2,550 m above the sea level (data derived from DEM 90×90 m). The mean slope and the river network density of the basin are 24.2% and 0.41 km/km^2 respectively. The main surface materials in the basin are granite, and granodiorite bed rocks, deluvial, alluvial sand - silt - clay deposit.

In the study area, there are only four rain gauges, among those only one collects hourly data; one climatic station at Tra My; and one discharge gauge at Nong Son. In general, the hydro-meteorological station network is poorly distributed since the rain gauges are installed every 800 km^2. The data were provided by the Hydro-Meteorological Data Center (HMDC) of the Ministry of Natural Resources and Environment (MONRE) of Vietnam.

Due to the effects of predominating wind direction (north-east in the rainy season) and topography, rainfall in the basin is very high and significantly varies in space and time. According to the rainfall records from 1980 to 2004 year, the rainfall distribution spatially increases from the East to the West and from the North to the South (the mean annual rainfall at Tra My station is more than 4,000 mm, whereas at Thanh My station is just more than 2,200 mm).

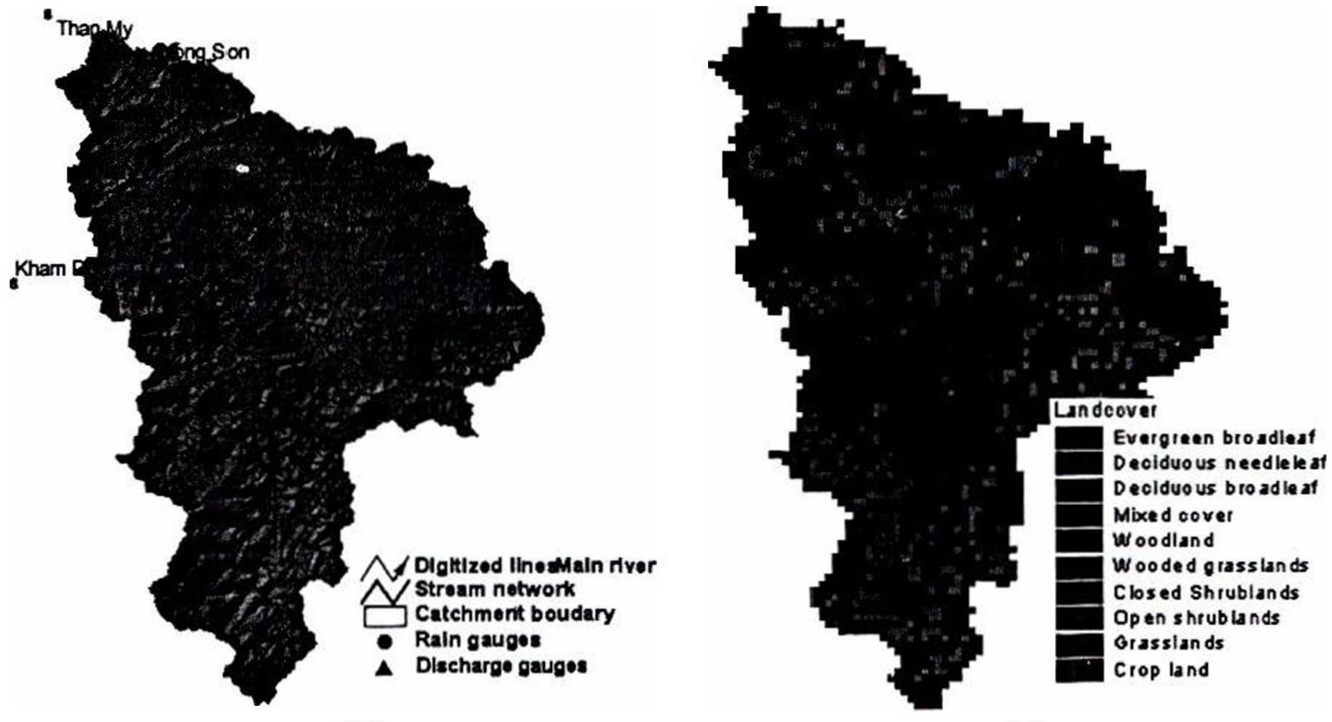

(a) (b)

Fig. 2. Nong Son catchment (a), and land covers map from UMD 1 km Global Land Cover (b).

For seasonal rainfall distribution, the rainfall in October and November reaches up to 1,800 mm. The period of the north-east wind lasts from September to December, coinciding with the rainy season on the basins. Although the rainy season only lasts just for 4 months, it contributes 70% of the annual rainfall. Furthermore, the annual rainfall also varies from 2,417 mm (1982) to 6,259 mm (1996) with an average value of 3,697 mm. The annual runoff coefficient (runoff / precipitation) in this period intensively varies between 0.49 (1982) and 0.81 (1995) with an average value of 0.73.

3.2. Land cover data and vegetation-related parameters

The land cover data was obtained from UMD 1km Global Land Cover (http://www.geog.umd.edu/landcover/1km-map.html) based on AVHRR and LDAS (Land Data Assimilation System) information. AVHRR provides information on globe land classification at 30 s resolution [13]. Fig. 2.b shows the vegetation classification at 30 s resolution for the Nong Son catchment. In this area, there are ten categories of land cover in which evergreen broadleaf occupies a largest area of 48.7% in total, followed by deciduous needleleaf: 19.3%, wooded grasslands: 18.0%, deciduous broadleaf: 4.2%, woodland: 3.3%, mixed cover: 3.2%, closed shrublands: 2.0%, open shrublands: 0.6%, grasslands: 0.4%, and crop land: 0.2%.

For each type of vegetation in the Nong Son catchment, the vegetation parameters, such as minimum stomata resistance, leaf-area index, albedo, and zeroplane displacement, are derived from http://www.ce.washington.edu/pub/HYDRO/cherkaue/VIC-NL/Veg/veg_lib; these data are presented in Table 1.

Table 1. Vegetation-related parameters for each type of vegetation in the Nong Son catchment

Vegetation classification	Albedo	Minimum stoma resistance (s/m)	Leaf area index	Roughness length (m)	Zero-plane displacement (m)
Evergreen broadleaf forest	0.12	250	3.40–4.40	1.4760	8.040
Deciduous needleleaf forest	0.18	125	1.52–5.00	1.2300	6.700
Deciduous broadleaf forest	0.18	125	1.52–5.00	1.2300	6.700
Mixed forest	0.18	125	1.52–5.00	1.2300	6.700
Woodland	0.18	125	1.52–5.00	1.2300	6.700
Wooded grasslands	0.19	135	2.20–3.85	0.4950	1.000
Closed shrublands	0.19	135	2.20–3.85	0.4950	1.000
Open shrublands	0.19	135	2.20–3.85	0.4950	1.000
Grasslands	0.20	120	2.20–3.85	0.0738	0.402
Croplands	0.10	120	0.02–5.00	0.0060	1.005

3.3. Meteorological data

In the Penman-Monteith method, the meteorological data, such as mean temperature, relative humidity, sunshine hour, and wind speed, are required. The observed data from the Tra My climatic station for the period of 1980-2004 were used in this study.

- Air temperature (*T*): The research basin is located in the monsoon tropical zone. Based on the data at Tra My station, it shows an average annual temperature of 24.5°C. The average lowest temperature during December-February ranges from 20 to 22°C with an absolutely minimum of 10.4°C, and the average highest temperature during a long period (April to September) ranges from 26 to 27°C with an absolutely maximum value of 40.5°C.

- Relative humidity (*RH*): The study area lies in a mountainous tropical humidity zone, and as such the value of relative humidity is fairly high and stable with an average value of 87%. The observed data show that the maximum humidity is observed in October to December, reaching 92%, while the minimum is observed somewhere between April and July, getting as high as 83% or more.

- Sunshine hours (*n*): Because it lies in the high rainy sub-region, the sunshine hours in the study area are relatively lower than those in the surrounding areas with a mean annual value of 5.1 hours/day. The monthly average of sunshine hours varies from 2.0 hours/day in December to 7.0 hours/day in May.

- Wind speed and direction (*u*): The popular directions of wind are south-east and south-west from May to September, east and north-east from October to April. The wind speed is moderate with an average annual value of 0.9 m/s.

4. Results and discussion

From the land cover data and vegetation-related parameters in the Nong Son catchment, and the monthly meteorological data at the Tra My climate station for the period of 1980-2004, the potential evapotranspiration values were determined by using the Penman-Monteith model. Table 3 and Fig. 3 show the calculation results of monthly potential evapotranspiration.

Table 2. Monthly average meteorological characteristics in the Nong Son catchment

Characteristics	Jan	Feb	Mar	Apr	May	Jun	Jul	Aug	Sep	Oct	Nov	Dec	Ave.
T (°C)	20.6	21.9	24.0	26.2	26.9	27.1	27.1	26.9	25.9	24.4	22.6	20.6	24.5
RH (%)	89.4	87.6	84.6	82.8	84.1	83.8	83.4	84.1	87.6	90.4	92.5	92.4	86.9
n (hours/day)	3.5	4.7	5.9	6.5	6.9	6.6	6.7	6.3	5.2	3.9	2.6	2.0	5.1
u (m/s)	0.8	1.1	1.0	0.9	0.8	0.8	0.8	0.8	0.8	0.9	0.8	0.7	0.9

Table 3. Calculated monthly mean potential evapotranspiration for each vegetation type and average over basin in the Nong Son catchment

ET (mm)	Jan	Feb	Mar	Apr	May	Jun	Jul	Aug	Sep	Oct	Nov	Dec	Annual
Evergreen broadleaf	56	63	93	111	123	122	129	123	99	75	54	47	1094
Deciduous needleleaf	53	56	87	124	147	142	149	141	108	84	55	47	1195
Deciduous broadleaf	53	56	87	124	147	142	149	141	108	84	55	47	1195
Mixed cover	53	56	87	124	147	142	149	141	108	84	55	47	1195
Woodland	53	56	87	124	147	142	149	141	108	84	55	47	1195
Wooded grasslands	58	68	108	131	137	130	137	128	106	83	59	49	1194
Closed shrublands	56	66	105	129	135	127	134	126	104	81	57	48	1170
Open shrublands	56	66	105	129	135	127	134	126	105	86	62	53	1186
Grasslands	63	74	108	124	132	125	131	125	105	86	62	53	1188
Crop land	20	9	32	92	123	123	134	132	101	54	22	10	853
Areal	56	62	94	119	133	129	136	129	103	79	55	48	1144

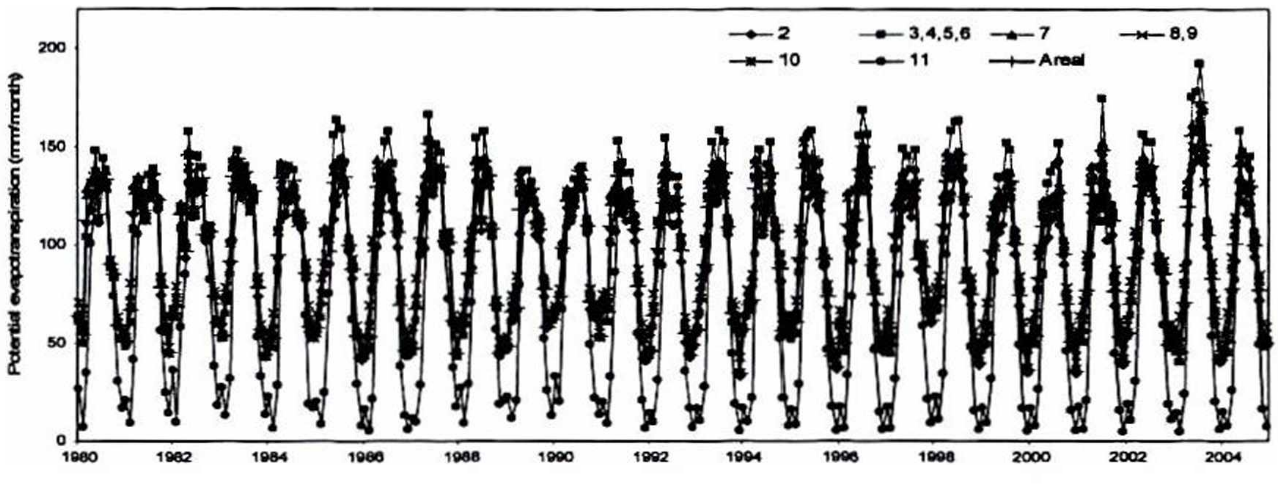

Fig. 3. Calculated monthly potential evapotranspiration for each type of vegetation and average over basin in the Nong Son catchment for the 1980-2004 period. Note: 2- Evergreen broadleaf; 3, 4, 5, 6 - Deciduous needleleaf, Deciduous broadleaf, Mixed cover, and Woodland; 7 - Wooded grasslands; 8, 9 - Closed shrublands, and Open shrublands; 10 - Grasslands; 11- Crop land; and Areal-Average potential evapotranspiration over basin.

Table 4. Monthly mean potential evapotranspiration estimated by using the Penman-Montheith method and Piche tube data in the Nong Son catchment for the period of 1980-2004

ET (mm)	Jan	Feb	Mar	Apr	May	Jun	Jul	Aug	Sep	Oct	Nov	Dec	Annual
ET_{P-M}	56	62	94	119	133	129	136	129	103	79	55	48	1144
ET_{Piche}	68	82	118	119	133	120	128	125	103	84	62	56	1198

Based on the result of Southern Institute of Water Resources Research [27], the potential evapotranspiration was derived from Piche tube observation values while multiplying it by correction factors, this is usually called ET_{Piche}.

The comparative performance of ET by the Penman-Monteith method (ET_{P-M}) and ET_{Piche} during the 1980-2004 period, Table 4 shows a relatively small difference in the annual value, precisely less than 5%. However there is difference in monthly distribution, particularly from January to March with $ET_{Piche} > ET_{P-M}$ of about 27%. Based on the climatic characteristics in Table 2, ET_{P-M} shows a closer accord with the seasonal distribution. Fig. 4 shows that ET_{Piche} values are somewhat unrealistic, for example, potential evaporation in June 1985 has an average value of 7 mm/day which is too high for any natural tropical humid area. This result agrees with that of Nguyen [4] that the observed Piche data often give erroneous outputs.

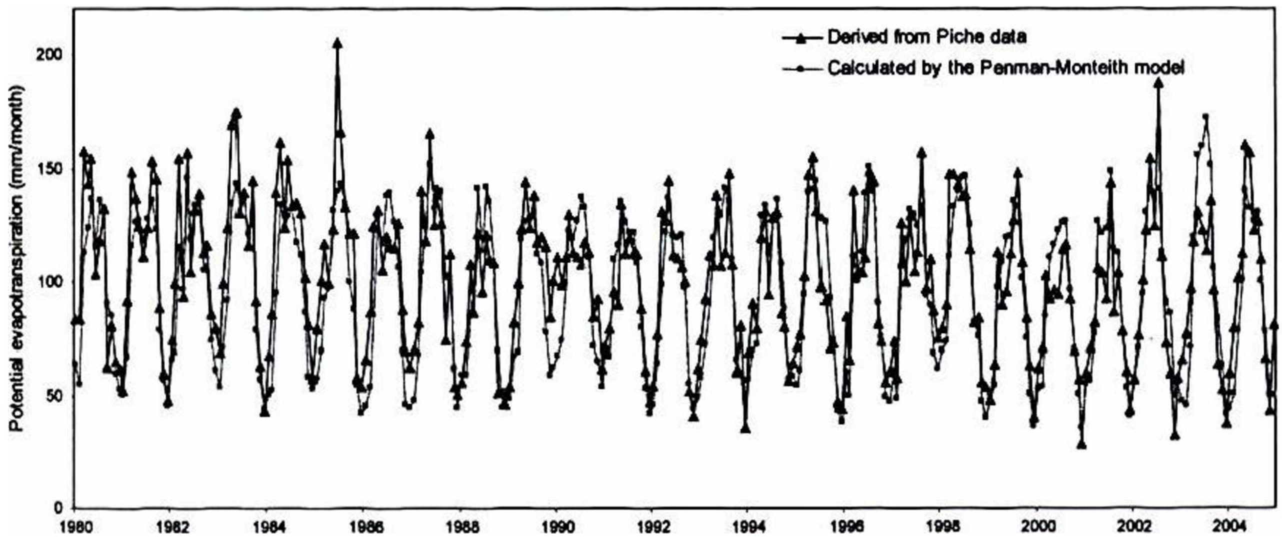

Fig. 4. Comparison of monthly potential evapotranspiration estimated by the Penman-Monteith method and Piche tube data in the 1980-2004 period.

In order to assess further the suitability of the potential evapotranspiration estimated directly by using the Penman-Monteith method and that derived from the Piche data, the NAM conceptual model was used to simulate the hydrology of the study area in the 1983-2003 period. The NAM model performance is evaluated with a set of two statistical criteria: bias and Nash-Sutcliffe efficiency coefficient [22].

Table 5. Performance measures of two potential evapotranspiration inputs during the simulation period (1983-2003) for the Nong Son catchment

Performance statistics	ET_{P-M}	ET_{Piche}
Bias (%)	3.100	-2.636
Nash-Sutcliffe efficiency, R^2	0.880	0.802

Discharge simulated by using the input data of ET_{Piche} and ET_{P-M} is shown as monthly averages in Fig. 5. Performance measures are given in Table 5. While the overall simulated discharge with the input of ET_{P-M} is slightly smaller than the observed one, in the case of ET_{Piche} it is the reverse. However, the overall water balances (bias) in both cases are realistic (less than 5%). The good thing here is that ET_{P-M} provides a better model performance in the term of the Nash-Sutcliffe efficiency (0.880) against that of ET_{Piche} (0.802) with respect to the model simulation of the discharge at the stream gauge.

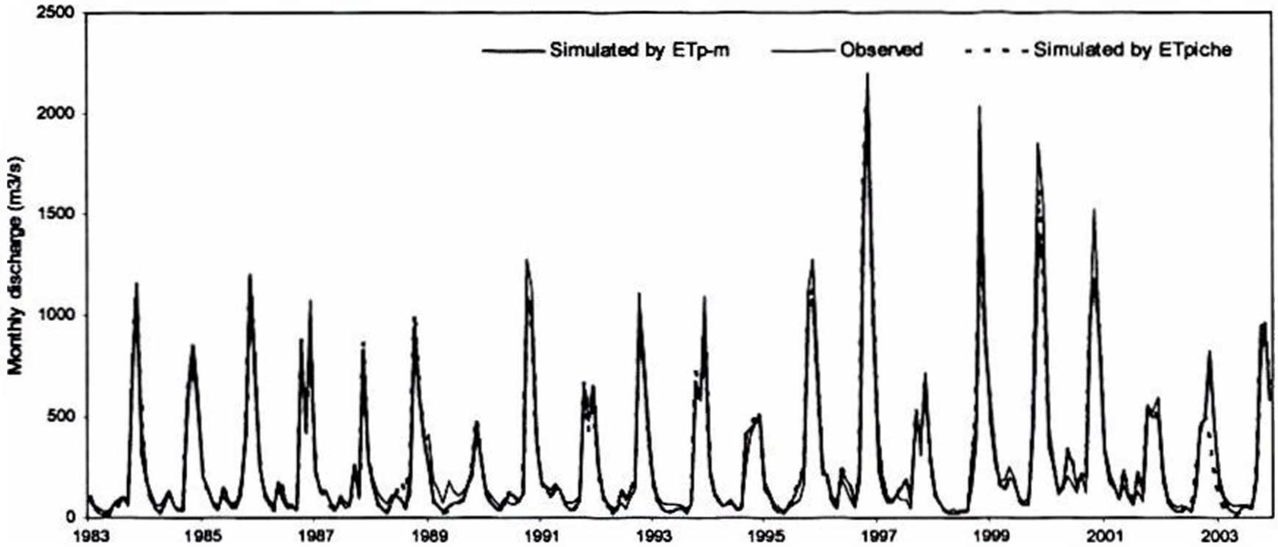

Fig. 5. Observed vs. simulated monthly discharges for the 1983-2003 period using the potential evapotranspiration inputs of ET_{Piche} and ET_{P-M}.

5. Conclusions

The Penman-Monteith method was used to compute directly the potential evapotranspiration for the Nong Son catchment. The approach was assessed the suitability through the hydrological model response performance. The result of this approach shows a close agreement between the simulated and observed discharges at the stream gauge in comparison with Piche observation. The main conclusion here is that the Penman-Monteith evapotranspiration is more reliable than the Piche method as well as using pan data. Although the approach requires the data on land cover and vegetation-related parameters, these data are available on internet in recent years. Hence, due to the importance of evapotranspiration in water balance, the Penman-Monteith method is recommended as the sole standard method to apply for similar catchments.

Acknowledgements

The authors would like to thank the Danish Hydraulic Institute (DHI) for providing the NAM software license, and the Southern Institute of Water Resources for data support.

References

[1] R.G. Allen, A penman for all seasons, *Jour. of Irr. & Drainage Engineering* 112(1987) 348.

[2] R.G. Allen, Irrigation engineering principles, Utah State University, *Utah* 12 (1995) 108.

[3] R.G. Allen, L.S. Pereira, D. Raes, M. Smith, *Crop evapotranspiration-guidelines for computing crop water requirements*, FAO Irrigation and Drainge Paper 56, Rome, 1998.

[4] N.N. Anh, *The evaluation of water resources in the Eastern Nam Bo*, Project KC12-05, Southern Institute for Water Resources Planning, Ho Chi Minh City, 1995 (in Vietnamese).

[5] W. Brutsaert, Comments on surface roughness parameters and the height of dense vegetation, *J. Meteorol. Soc. Japan* 53 (1975) 96.
[6] W. Brutsaert, Heat and mass transfer to and from surfaces with dense vegetation or similar permeable roughness, *Boundary - Layer Meteorology* 16 (1979) 365.
[7] W. Brutsaert, *Evaporation into the atmosphere*, D. Reidel Pub. Co., Dordrecht, Holland, 1982.
[8] Danish Hydraulic Institute, *NAM calculation materials*, Horsholm, Denmark, 2003.
[9] Danish Hydraulic Institute, *MIKE 11*, Horsholm, Denmark, 2004.
[10] P.J.M. De Laat, H.H.G. Savenije, *Principle of hydrology*, Lecture note, IHE, Deft, 2000.
[11] C.A. Federer, C.J. Vorosmarty, B. Fekete, Intercomparison of methods for potential evapotranspiration in regional or global water balance models, *Water Resour. Res.* 32 (1996) 2315.
[12] J.R. Garrat, B.B. Hicks, Momentum, heat and water vapour transfer to and from natural and artificial surface, *Quarterly Journal of the Royal Meteorological Society* 99(1973) 680.
[13] M. Hansen, R. DeFries, J.R.G. Townshend, R. Sohlberg, Global land cover classification at 1km resolution using a decision tree classifier, *International Journal of Remote Sensing* 21 (2000) 1331.
[14] P. Irannejad, Y. Shao, Description and validation of the atmosphere-land-surface interaction scheme (ALSIS) with HAPEX and Cabauw data, *Global and Planetary Change* 19 (1998) 87.
[15] P.G. Jarvis, The interpretation of the variation in leaf water potential and stomatal conductance found in canopies in the field, *Philosophical Transactions of the Royal Society of London Series* B 273 (1976) 593.
[16] H.T.H. Kirnak, T.H. Short, An evapotranspiration model for nursery plants grown in a lysimeter under field conditions, *Turk J Agric For* 25 (2001) 57.
[17] D.R. Maidment, *Handbook of hydrology*, MacGraw-Hill, New York, 1993.
[18] P. Maisongrande, A. Ruimy, G. Dedieu, B. Saugier, Monitoring seasonal and interannual variations of gross primary productivity and net ecosystem productivity using a diagnostic model and remotely - sensed data, *Tellus B* 47 (1995) 178.
[19] X. Mo, S. Liu, Z. Lin, W. Zhao, Simulating temporal and spatial variation of evapotranspiration over the Lushi basin, *Journal of Hydrology* 285 (2004) 125.
[20] J.L. Monteith, Evaporation and environment, *Symp. Soc. Exp. Bio.*, Cambridge University Press, Cambridge, XIX (1965) 205.
[21] J.L. Monteith, Evaporation and surface temperature, *Quarterly Journal of the Royal Meteorological Society* 107 (1981) 1.
[22] J.E. Nash, J.V. Sutcliffe, River flow forecasting through conceptual models, Part I: A discussion of principles, *J. Hydrol.* 10 (1970) 282.
[23] H.L. Penman, Natural evaporation from open water, bare soil and grass, *Proc. Royal Soc.* London, A193 (1948) 120.
[24] P.J. Sellers, J.A. Berry, G.J. Collatz, C.B. Field, F.G. Hall, Canopy reflectance, photosynthesis and transpiration, Part III: A re-analysis using improved leaf models and a new canopy integration scheme, *Remote sens. Environ.* 42 (1992) 187.
[25] P.J. Sellers, S.O. Los, C.J. Tucker, C.O. Justice, D.A. Dazlich, G.J. Collatz, D.A. Randall, A revised land surface parameterization (SiB2) for atmospheric GCMs, Part II. The generation of global fields of terrestrial biophysical parameters from satellite data, *Journal of Climate* 9 (1996) 706.
[26] J.B. Stewart, Modelling surface conductance of pine forest, *Agricultural and Forest Meteorology* 43 (1988) 19.
[27] SWECO International, *Song Bung 4 hydropower project*, TA No.4625-VIE, Vietnam, 2006.
[28] O. Tetens, Uber einige meteorologische Begriffe, *Z. Geophys.* 6 (1930) 203.
[29] C.W. Thornthwaite, An approach toward a rational classification of climate, *Geographical Rev.* 38 (1948) 55.
[30] P.J. Vanderkimpen, *Estimation of crop evapotranspiration by means of the Penman-Monteith equation*, Ph.D. thesis, Utah State University, 1991.
[31] D.L. Verseghy, N.A. McFarlance, M. Lazare, CLASS-a Canadian land surface scheme for GCMs. II. Vegetation model and coupled runs, *International Journal of Climatology* 13 (1993) 347.
[32] C.J. Vorosmarty, C.A. Federer, A.L. Schloss, Potential evaporation functions compared on US watersheds: possible implications for global-scale water balance and terrestrial ecosystem modeling, *J. Hydrol.* 207 (1998) 147.
[33] M.C. Zhou, H. Ishidaira, H.P. Hapuarachchi, J. Magome, A.S. Keim, K. Takeuchi, Estimating potential evapotranspiration using the Shuttleworth-Wallace model and NOAA-AVHRR NDVI to feed a distributed hydrological modeling over the Mekong River Basin, *J. Hydrol.* 327 (2005) 151.